Molecular Crystals and Liquid Crystals

Publication details, including instructions for authors and subscription information:
http://www.tandfonline.com/loi/gmcl20

Conducting Polymer and Conducting Composite Strain Sensors on Textiles

Paul Calvert [a], Deepak Duggal [a], Prabir Patra [a], Animesh Agrawal [a] & Amit Sawhney [a]

[a] Department of Materials and Textiles, University of Massachusetts Dartmouth, MA, USA

Version of record first published: 22 Sep 2010

To cite this article: Paul Calvert, Deepak Duggal, Prabir Patra, Animesh Agrawal & Amit Sawhney (2008): Conducting Polymer and Conducting Composite Strain Sensors on Textiles, Molecular Crystals and Liquid Crystals, 484:1, 291/[657]-302/[668]

To link to this article: http://dx.doi.org/10.1080/15421400801904690

Mol. Cryst. Liq. Cryst., Vol. 484, pp. 291/[657]–302/[668], 2008

ISSN: 1542-1406 print/1563-5287 online
DOI: 10.1080/15421400801904690

Taylor & Francis
Taylor & Francis Group

Conducting Polymer and Conducting Composite Strain Sensors on Textiles

Paul Calvert, Deepak Duggal, Prabir Patra, Animesh Agrawal, and Amit Sawhney
Department of Materials and Textiles, University of Massachusetts Dartmouth, MA, USA

Metallic connections and polymer sensors have been printed onto textiles as a step toward the production of flexible printed electronics. We show that the strain response of conducting polymers and composites on woven textiles depends on the detailed distribution the sensor material on the yarn. The structure of most textiles, with strong fibers twisted into yarns, can provide a support which allows electronic materials, impregnated into the yarn, to stretch and bend without breaking.

Keywords: inkjet printing; strain sensors; textiles

INTRODUCTION

Metal and semiconductor strain gauges are familiar in engineering. They withstand strains of a fraction of a percent and a few percent respectively. In developing "smart textiles" and other soft devices and machines, we would like to utilize electrical connections and sensors that function at much larger strains.

Conducting polymers are an attractive choice for these sensors, they have a high resistance, are flexible and can easily be printed. There have been past studies of polypyrrole and polyaniline gas sensors [1-3]. More recently, strain sensors have been used in a number of formats, including strips of Lycra elastic fabric impregnated with conducting polymer [4] and impregnated foams as compression sensors for shoes [5].

Address correspondence to Paul Calvert, Department of Materials and Textiles, University of Massachusetts, Dartmouth, N. Dartmouth, MA 02747, USA. E-mail: pcalvert@umassd.edu

Our work uses multi-pass inkjet printing [6] to deposit sensing lines of conducting polymer on fabric and to print silver lines to connect the sensors to the monitoring equipment. We use an electroless plating method but a two-step printing method for silver has also been described [7]. The performance of these strain sensors depends on distribution of the conducting polymer through the fabric and on the weave of the fabric.

Among the conducting polymers, several polythiophenes combine processability and environmental stability. Poly(3,4-ethylenedioxythiophene)-poly(styrenesulfonate) (PEDOT-PSS) shows high conductivity, transparency and possesses great environmental stability. It is readily available as an aqueous suspension of the conjugated polymer in combination with a soluble polyelectrolyte, poly (styrene sulfonic acid) (PSS), as a charge balancing dopant and dispersant. In order to deposit both the sensors and the connecting conductors onto the fabric, we have used inkjet printing [6,8]. The connections are printed metal lines with a resistance much less than that of the conducting polymer sensor, such that any change in resistance of the connectors with strain is insignificant compared to that of the sensors.

As an alternative to conducting polymers we have also investigated the strain response of printable conducting composites. This system is based on water-soluble epoxides and amines that can be printed or deposited as a hydrogel containing carbon black at a sufficient level to be conducting [9,10].

We envisage these sensors being printed in arrays onto textiles in order to monitor the motions of an athlete or a patient in rehabilitation, for instance.

EXPERIMENTAL

The Inkjet Printing System

Printing was carried out using conventional HP cartridges, emptied and refilled with our test solutions. The drop rate was controlled by a custom-built pulse generator which pulsed a single nozzle on the cartridge. The cartridge was mounted on an arm above an xy motion system that moves the samples, Figure 1. In this way, many print cycles could be carried out with controlled time and distance between drops and with the ability to control the temperature and humidity of the sample.

Formation of Connectors

Formation of conducting leads was attained in two steps. The first was to inkjet print seed layers which were then converted into metallic lines by electroless plating.

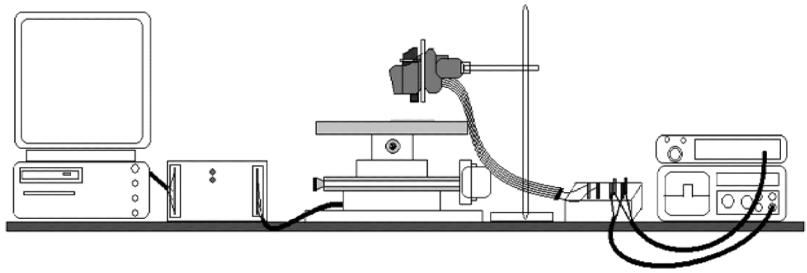

FIGURE 1 Inkjet printing assembly.

0.32 gms of silver nitrate, dissolved in 50 ml of water was printed on the woven fabric.

Since the ink, upon evaporation, leads to spreading on the substrate the woven fabric was mounted on a heating plate so as to avoid the spreading of the solution. This technique allows the individual droplets to fuse but hinders the formation of large droplets and thus prevents smearing of ink [8]. Lines were printed at 5 cm/sec and 500 drops/sec for 500 cycles. This repeated printing onto fabric at 80°C allows the "ink" to dry on the fabric between cycles. Once the lines, 3 cm long and 0.5 mm wide, are printed, the sample was dipped in an electroless bath of silver [11]. The reducing agent, glucose, reduces the silver ions to metal which is deposited on to the already printed seed layer by an autocatalytic process.

The bath was maintained at a temperature of 50°C and the hold time of 40 minutes. The pH of the bath was kept highly basic at around 12.5. After the sample is subjected to the required set of conditions, it is taken out of the bath and rinsed in hot water followed by a rinse in cold water along with mechanical action such as wringing. A thick and uniform deposit of silver nitrate formed on the nylon woven fabric.

The resistance of the samples, after they have dried, was measured using Keithley 196 electrometer and also by 4-point electrical measurements that eliminate the effect of the terminal resistance. The probes were kept on the printed region, and the corresponding reading from the front panel is taken down. The value of resistance ranges from 0.7–1.5 ohms/inch. Based on the linewidth, fabric thickness and volume fraction of silver, we estimate a conductivity of approximately 4×10^3 Siemens/cm. This is about 100 times less than that of elemental silver (6.25×10^5 Siemens/cm). Unprinted areas of the fabric remain non-conductive.

Formation of PEDOT Sensors

A suspension of PEDOT-PSS (Bayer Scientific), 1.3% by weight, was printed onto the fabric for 500 cycles at 5 cm/sec and 500 drops/sec. The printed lines were about 5 cm long and less than 1 mm wide. The samples were annealed at 90°C for about an hour. In this case the polymer partly penetrated the fabric and formed stable conducting lines. The resistance drops as more ink is deposited and is about 5 kiloohms at 500 cycles. The conductivity of the PEDOT in the coatings is about 25 S/cm.

For the strain sensing study, the fabric was clamped in jaw placed 2.54 cm apart on an Instron tensile testing machine and the corresponding resistance was recorded on a Keithley Multimeter 196 through a PC using General Purpose Interface Bus (GPIB) as a data acquisition mode.

The microstructure of the printed PEDOT and electroless silver was studied by JEOL JSM 5610 Scanning electron microscope equipped with Oxford Instruments Energy Dispersive X-ray System operating at 8 kV.

Gel Sensors

Gels based on water-soluble aliphatic polyamines and polyetheramines reacted with aqueous solutions of polyethyleneglycol diglycidylether (PEGDGE) were prepared [9,10]. Carbon black 10 wt% was added to make the gels conductive close to the percolation threshold. Amine-cured epoxy networks are mostly formed from the epoxide-amine addition reaction which is shown in Figure 2. An amine hydrogen/epoxy stoichiometry of 2.5:1 was used, this was chosen to give a soft, tough gel. Steric interference slows the reaction rate of the secondary amines as compared to the unreacted primary amines. Hence most of the remaining amine hydrogens on the final network will be secondary amines. The pre-cured gel was written with a fine needle onto the test fabric, Figure 3.

Integration of Sensors and Connectors

Resistance of connectors was 1/100 of that of sensor in order to avoid any interference with the data recording. Sensors were integrated with connectors by printing lines of PEDOT, 1 cm in length and about 0.5 mm wide, onto Nylon 66 fabrics in between silver printed lines, as shown in Figure 4. The connectors were connected to an external device and the resistance was recorded on Keithley 196 electrometer along, interfaced through GPIB.

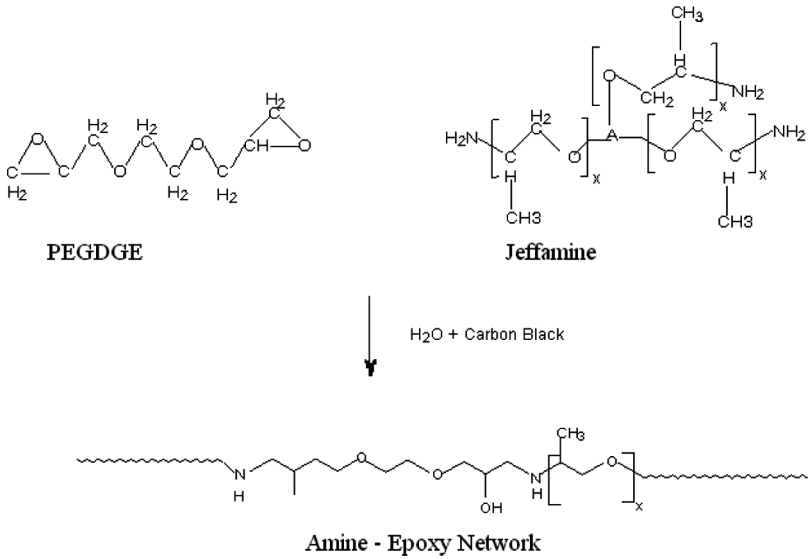

FIGURE 2 Gel formation.

RESULTS AND DISCUSSION

For the printed silver connectors, Figure 5, shows a coating of silver around every fiber through the thickness of the fabric. The printed PEDOT, likewise shows conducting polymer distributed around each

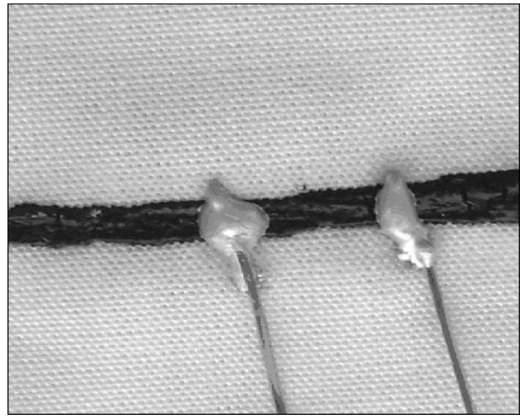

FIGURE 3 Conducting gel sample, 1 cm long, on fabric, with connecting leads.

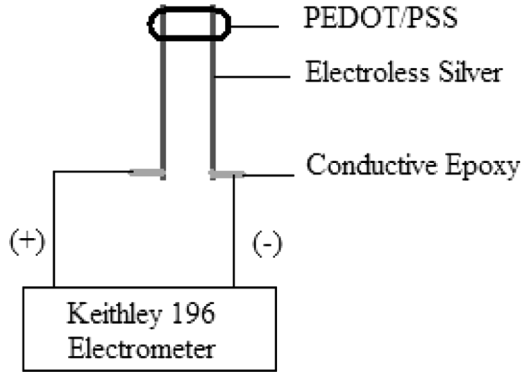

FIGURE 4 Integration of sensors (PEDOT-PSS) with connectors (Electroless silver).

fiber [12] as well as a solid layer of polymer on the fabric surface, Figure 6.

The reversible change in the electrical resistance of PEDOT-PSS printed fabrics with external mechanical strain relaxation reveals that these fabrics show piezoresistivity. For this study 2.54 cm long PEDOT printed cotton fabric was subjected to an elongation of 5% at a rate of 5 mm/min on an Instron tensile testing machine, Figure 7.

It can be seen that there is an initial increase in the resistance of the PEDOT printed fabric with strain. We believe that this initial increase corresponds to the cracking seen in Figure 6 and reported by Li *et al*. for Lycra fabric with a coating of polypyrrole [13,14]. Subsequently our samples show a cyclic change in resistance with strain. In this case the resistance decreases as the sample is strained and increases again as the strain is relaxed. It can be seen that a strain of 5% results in a resistance decrease of about 25%, corresponding

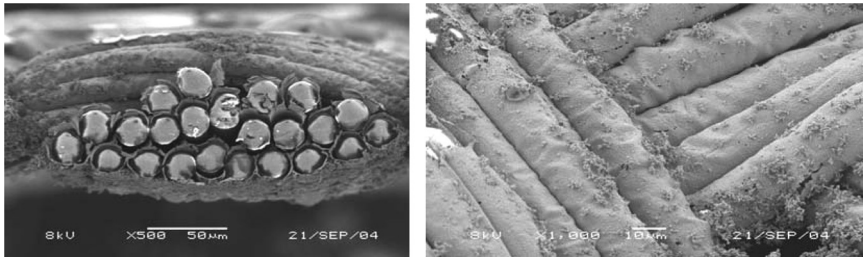

FIGURE 5 Cross section and top view of silver printed region of a Nylon fabric.

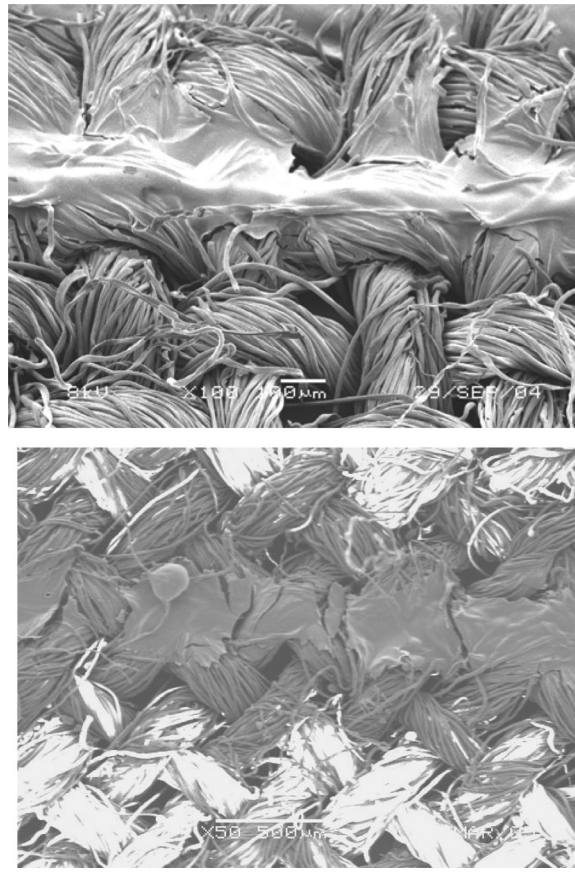

FIGURE 6 PEDOT-printed cotton before and after 10% elongation.

to a (negative) gauge factor of -5. A similar large decrease in resistance with strain was observed for polypyrrole-impregnated Lycra [4]. This compares with a gauge factor of $+2$ for most metals, which reflects the normal decrease in cross-section with increase in length. Some semiconductors do show a large positive gauge factor due to the influence of strain on band conductivity [15]. Our samples thus show two zones of conductivity. The surface layer of conducting polymer cracks on stretching while the polymer that penetrates into the yarn becomes more conductive on stretching, probably through better surface-surface contacts within the yarn [16]. The flat section of each wave on the upper, high resistance, section was attributed to slow strain recovery. Cotton woven fabric which shows only 61% of recovery from strain as

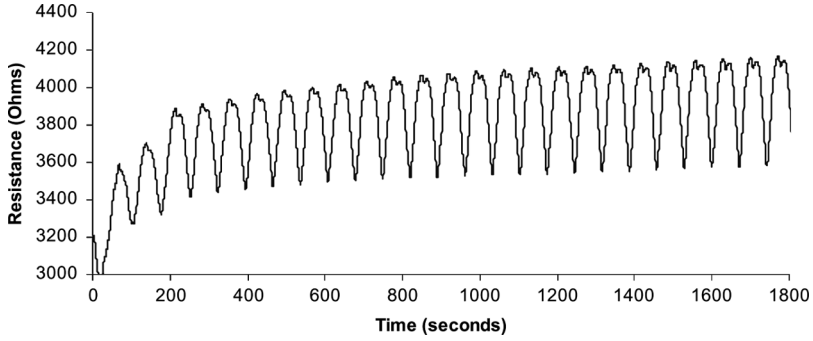

FIGURE 7 Resistance of PEDOT-PSS sensor with 25 repeated cycles of strain to 5% and relaxation.

compared to Nylon fabric (91%) and some knit fabrics (almost 100%), although with time original resistance is recovered.

As mentioned above, the printed PEDOT shows a two-stage response to strain. Over the first few cycles, the resistance increases as the surface layer, shown in Figure 6, cracks. Subsequently the material shows a stable response over many cycles. This response is a decrease of resistance with increasing strain, with a flattened top to each cycle as the fabric becomes relaxed.

The mechanics of a woven fabric are complex, but much of the response to tensile strain is in untwisting of the individual short (staple) filaments within the yarn in the manner of a twisted telephone cord [17]. This untwisting is accompanied by lateral compression between the filaments. Thus, if we view each short filament as being coated with conductor, the decrease in resistance is due to compressive stresses increasing fiber-fiber contact. One expected consequence of this model would be that low-twist, loose yarns would show more response for a given strain as the fibers more into much closer contact. The response of a fabric may, of course, be more complicated as yarns also move within the fabric.

Table 2 shows measured gauge factors for different fabrics specified in Table 1, test directions relative to the main fabric axis and relative to the line direction, and test speed. multiple tests on signle samples and multiple samples of similar sensors show good reproducibility for gauge factor within 10%. It can be seen that the twill fabric and the plain fabric tested on the fabric diagonal give especially high negative values.

The thicker, coarser twill fabric shows a greater response as contacts are initially poor. This fabric also shows a higher gauge factor

TABLE 1 Fabric Specifications

	Yarn count	Construction	Weight g/m^2	Twist/inch
Cotton twill	14.75/1 warp & fill	106×56	258	17 warp and fill
Cotton poplin	20/1 warp, 17/1 fill	80×50	180	15 warp, 13 fill
Combed cotton warp sateen	40/1 warp, 30/1 fill	130×70	155	27 warp, 22 weft

TABLE 2 Sensor Gauge Factor

	Gauge factor				
	Sensor line angle to fabric axes			Tension diagonal to line	High speed
	0°	45°	90°		
Plain	6.00	9.50	5.50	14.00	7.50
Twill	12.00	9.00	11.50	9.50	12.00
Sateen	6.00	6.80	6.00	7.00	9.90

for lines printed across the fabric axes where contact at yarn-to-yarn crossing points is also important. For the diagonal tests, the line is parallel to the fabric axes but the tension direction is at 45 degrees to the line. This response then reflects a combination of tension and shear on the line. These differences are potentially important as an ideal sensor would be able to distinguish strains on different axes.

Gel Sensors

Figures 8 and 9 show the response of the written gel sensors at 10% and 15% strain. These materials are not embedded within the fabric, a plain cotton poplin, but are on the surface, unlike the brittle conducting polymers, these gels do withstand strains up to 15% and so do not need the support provided by the twisted yarn structure. At 10% strain the gauge factor is roughly -2. The low value suggests a conventional response to volume change on strain, similar to the gauge factor of 2 for metal strain gauges. The fact that the factor is negative suggests that the restructuring of the composite gel is more complex than a simple shape change. At 15% strain, the gauge factor drops to 0.3 and the response curve is flattened on the high tension, low resistance side of each cycle. The chaotic response during the first two cycles shows that some permanent deformation of the gel occurs at strains above 10%.

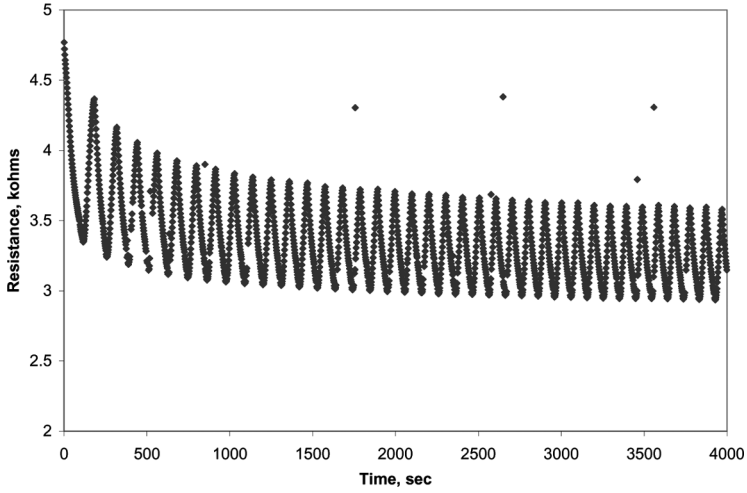

FIGURE 8 Response of gel sensor on cotton to 10% strain.

Identification of Human Motions

In order to explore the applicability of this system to analyzing joint motion, an assembly of sensors and connectors was placed on human knee, as shown in Figure 10, and wrist with the help of tape.

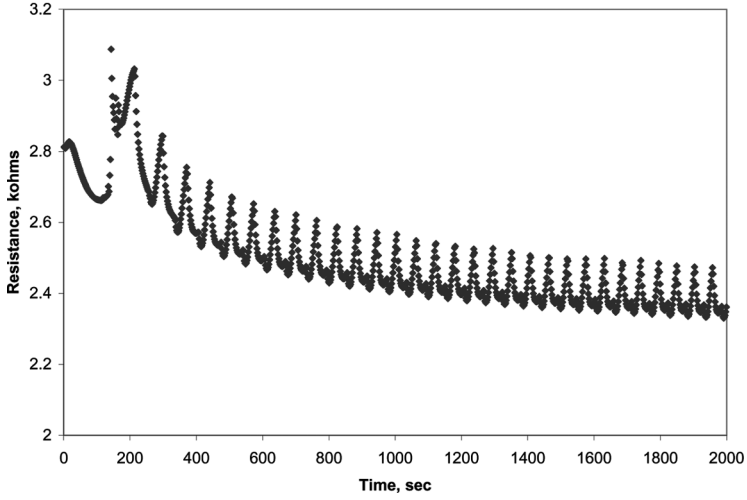

FIGURE 9 Response of gel sensor on cotton to 15% strain.

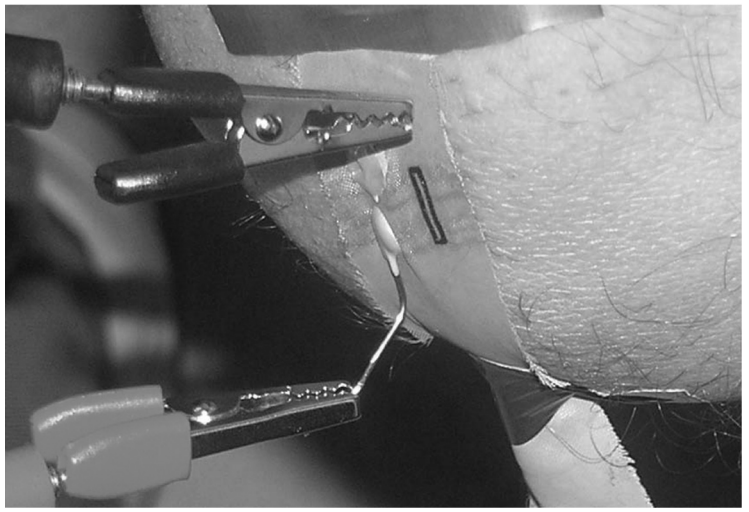

FIGURE 10 Sensor for bending of knee.

Four trials for each motion, bending of knee and twisting of wrist, was carried out at both slow and fast speed and corresponding change in resistance was recorded with the help of Keithley 196 Electrometer and GPIB. Both time and frequency domain analysis was carried out of the readings as a part of digital signal processing.

To reduce the noise in the original data a mean filter was employed. This is a simple sliding-window spatial filter that replaces the first value in the window with the average (mean) of all the data values in the window. The plots, shown in Figure 11, are the two trials after

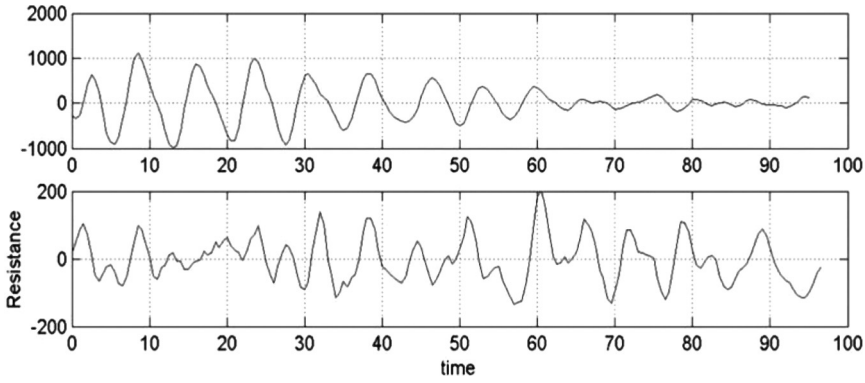

FIGURE 11 Sensor resistance during knee bending after removing running average and 2nd mean filtering. 2 trials.

removing running average and taking twice mean filtering in the time domain. A pseudo-sinusoidal wave is shown in the data after doing signal processing. Approximate 7 pseudo-sinusoidal cycles are contained in 50 sec. In the frequency domain, existing data was used to estimate the power spectral density.

CONCLUSIONS

Printed conducting polymer piezoresistive strain sensors on fabrics can give a high negative gauge factor and so high sensitivity to small strains. Good performance derives from the polymer embedded within the yarn, while the surface layer cracks and becomes ineffective after one cycle of strain. The details of the sensing mechanism are unclear but it depends on improved fiber-to-fiber contact during tensile strain of the twisted yarns.

REFERENCES

[1] Armes, S., Aldissi, M., Hawley, M., Beery, J., & Gottesfeld, S. (1991). *Langmuir*, *7*, 1447–1452.
[2] Kuhn, H., Kimbrell, W., Fowler, J., & Barry, C. (1993). *Synthetic Metals*, *57*, 3707–3712.
[3] Kincal, D., Kumar, A., Child, A., & Reynolds, J. (1998). *Synthetic Metals*, *92*, 53–56.
[4] Wu, J., Zhou, D., Too, C., & Wallace, G. (2005). *Synthetic Metals*, *155*, 698–701.
[5] Brady, S., Lau, K., Megill, W., Wallace, G., & Diamond, D. (2005). *Synthetic Metals*, *154*, 25–28.
[6] Calvert, P. (2001). *Chem. Mater.*, *13*, 3299–3305.
[7] Bidoki, S. M., McGorman, D., Lewis, D. M., Clark, M., Horler, G., & Miles, R. E. (2005). *AATCC Review*, *5*, 11–14.
[8] Calvert, P., Yoshioka, Y., & Jabbour, G. (2004). Inkjet printing for biometric and biomedical materials. In: *Learning from Nature How to Design New Implantable Materials*, Weiner, R. L. R. S. (Eds.), Kluwer: 169–180.
[9] Yoshioka, Y. & Calvert, P. (2002). *Experimental Mechanics*, *42*, 404–408.
[10] Yoshioka, Y. & Calvert, P. (2001). *PMSE Preprints (ACS)*, *84*, 335–336.
[11] Korua, N. (1990). Electroless plating of silver. In: *Electroless Plating: Fundamentals and Applications*, Mallory, G. O. & Hajdu, J. B. (Eds.), Noyes Data Corporation: 441–461.
[12] Sawhney, A., Agrawal, A., Lo, T.-C., Patra, P. K., Chen, C. H., & Calvert, P. (2007). *AATCC Review*, *7*, 42–48.
[13] Li, Y., Cheng, X., Leung, M., Tsang, J., Tao, X., & Yuen, M. (2005). *Synthetic Metals*, *155*, 89–94.
[14] Li, Y., Leung, M., Tao, X., Cheng, X., Tsang, J., & Yuen, M. (2005). *J. Mater. Sci.*, *40*, 4093–4095.
[15] Eaton, W. & Smith, J. (1997). *Smart Materials & Structures*, *6*, 530–539.
[16] Zhang, H., Tao, X., Yu, T., Wang, S., & Cheng, X. (2006). *Meas. Sci. Technol.*, *17*, 450–458.
[17] Hearle, J., Grosberg, P., & Backer, S. (1969). *Structural Mechanics of Fibers, Yarns and Fabrics*, J Wiley: New York, Vol. 1.